Original Research

EPI-BOLD fMRI of Human Motor Cortex at 1.5 T and 3.0 T: Sensitivity Dependence on Echo Time and Acquisition Bandwidth

Francesco Fera, MD,[1,2] Martin N. Yongbi, PhD,[3] Peter van Gelderen, PhD,[3] Joseph A. Frank, MD,[4] Venkata S. Mattay, MD,[1] and Jeff H. Duyn, PhD[3]*

Purpose: To investigate the sensitivity dependence of BOLD functional imaging on MRI acquisition parameters in motor stimulation experiments using a finger tapping paradigm.

Materials and Methods: Gradient-echo echo-planar fMRI experiments were performed at 1.5 T and 3.0 T with varying acquisition echo time and bandwidth, and with a 4 mm isotropic voxel size. To analyze the BOLD sensitivity, the relative contributions of BOLD signal amplitude and thermal and physiologic noise sources were evaluated, and statistical *t*-scores were compared in the motor area.

Results: At 1.5 T, the number of activated pixels and the average *t*-score showed a relatively broad optimum over a TE range of 60–160 msec. At 3.0 T, an optimum range was observed between TEs of 30–130 msec. Averaged over nine subjects, maxima in the number of pixels and *t*-score values were 59% and 18% higher at 3.0 T than at 1.5 T, respectively, an improvement that was lower than the observed 100% to 110% increase in signal-to-noise ratio at 3.0 T.

Conclusion: The somewhat disappointing increase in *t*-scores at 3.0 T was attributed to the increased contribution of physiologic noise at the higher field strength under the given experimental conditions. At both field strengths, reducing the effective image acquisition bandwidth from 35 to 17 Hz per pixel did not affect or only marginally affect the BOLD sensitivity.

Key Words: BOLD; fMRI; brain; optimization; EPI
J. Magn. Reson. Imaging 2004;19:19–26.
Published 2003 Wiley-Liss, Inc.†

FUNCTIONAL MAGNETIC RESONANCE Imaging (fMRI) based on blood oxygen level dependent (BOLD) contrast (1) allows detection of neuronal activation through a number of physiologic processes. Although the underlying contrast mechanism of BOLD fMRI is, as of yet, not fully understood, in monkeys there is mounting evidence of a direct correlation between the amplitude of BOLD fMRI signals and neuronal activity as measured by local field potentials (2). In addition, in humans, some studies have reported good correlation of BOLD localization and functional organization in the human visual cortex (3,4).

BOLD contrast fMRI is generated at the venous side of the neurovasculature, where significant deoxyhemoglobin concentrations exist. The decrease in deoxyhemoglobin concentration during activation, attributed to an increase in cerebral blood flow (CBF), leads to an increased T_2* relaxation time constant, which results in signal increases in T_2*-weighted MRI. The magnitude of this T_2* effect is dependent on B_0 field strength, and on the geometric distribution and size of the vessels involved. Changes in T_2* can be measured with gradient-echo MRI, with contrast determined by echo time (TE). Optimal contrast can be achieved by adjusting TE to match the apparent tissue T_2* (5), which is determined by B_0 field strength, tissue characteristics, and macroscopic susceptibility effects.

Apart from physiologic factors, such as vascular geometry and dynamics, the contrast mechanisms as well as the sensitivity of BOLD fMRI are determined by a number of experimental factors, including the sensitivity of the MRI technique to detect subtle signal changes associated with BOLD contrast, as well as the robustness of the MRI acquisition technique in the presence of motion. The latter factor can be optimized by using single-shot MRI acquisition techniques such as echo-planar imaging (EPI) or spiral imaging (6–8). Sensitivity can be improved by going to higher magnetic field strength, e.g., 3.0 Tesla (9–11), 4.0 Tesla (12–14), or 7.0 Tesla (15,16). A further gain can be achieved by the use of dedicated MRI receiver coils (4). At given field strength and with fixed instrumentation, BOLD sensitivity in fMRI is also dependent on acquisition parameters such as voxel size (17,18), echo time (4–6,19–21), and acquisition bandwidth.

The sensitivity of a BOLD experiment is determined by the available BOLD contrast, relative to the experimental noise. The experimental noise results from sev-

[1]Clinical Brain Disorder Branch, National Institutes of Mental Health, NIH, Bethesda, Maryland.
[2]Institute of Experimental Medicine and Biotechnology, National Research Council, Cosenza, Italy.
[3]Advanced MRI, Laboratory of Functional and Molecular Imaging, National Institutes of Neurological Diseases and Stroke, NIH, Bethesda, Maryland.
[4]Laboratory of Diagnostic Radiology Research, Clinical Center, National Institutes of Health, Bethesda, Maryland.
*Address reprint requests to: J.H.D., Advanced MRI, Building 10, Room B1D724, National Institutes of Health, 9000 Rockville Pike, Bethesda, MD 20892. E-mail jhd@helix.nih.gov
Received January 30, 2003; Accepted September 22, 2003.
DOI 10.1002/jmri.10440
Published online in Wiley InterScience (www.interscience.wiley.com).

eral sources, including the intrinsic (thermal) noise inherent to the MRI signal reception, and noise generated by the measurement setup and physiologic processes unrelated to the activation paradigm. These effects result from tissue pulsations, subject motion, and instrumental instabilities. Since all of these noise sources, except thermal noise, have some TE dependence (18,22), the optimum sensitivity in BOLD fMRI is not necessarily found at TE = T_2*, the condition for maximum BOLD effect.

The thermal noise present in an MRI scan, relative to the image intensity, can be reduced by lowering the signal reception bandwidth per pixel. This is equivalent to increasing the duration of the signal acquisition window. In an EPI acquisition, the tradeoff is an increased level of artifacts (e.g., geometric distortions, resolution loss through T_2*-blurring) along with a potentially reduced BOLD contrast, since a larger part of the acquisition does not occur at optimal TE.

The experiments described below aim at investigating these tradeoffs, by performing a series of fMRI experiments at varying echo time (TE) and bandwidth. To evaluate the influence of these two parameters on a typical BOLD fMRI experiment, EPI acquisitions were performed during an activation experiment involving the motor cortex, using isotropic 4 mm resolution at magnetic field strengths of 1.5 and 3.0 Tesla. Sensitivity was determined from statistical scores, and the various noise sources were quantified.

MATERIALS AND METHODS

MRI

MRI studies were performed on 1.5 T and 3.0 T MR systems (General Electric, Milwaukee, WI) using quadrature head coil transceivers. With this hardware, the intrinsic signal-to-noise ratio of the 3.0 T system was 100% to 110% higher than the 1.5 T system, as measured on human brain and corrected for tissue relaxation. Both systems were equipped with identical gradients, capable of generating gradient fields of 4×10^{-2} T m^{-1} with a slew-rate of 180 T m^{-1}second^{-1}.

Prior to each scan session, volunteer subjects gave written informed consent to participate in the study, which was approved by the Intramural Review Board (IRB) at the National Institutes of Health. Earplugs were provided for hearing protection against the acoustic noise generated by the MRI gradient system.

A total of 24 functional neuroimaging motor stimulation experiments were conducted on nine normal subjects (five females and four males, mean age 28.7 ± 5) on both scanners, 13 at 1.5 T and 11 at 3.0 T. Some subjects were scanned twice in the same week. Their repositioning was based on scout images from the first session. To minimize inconsistency between sessions, standard home-built equipment was used at both fields to secure the volunteer's head in the same position within the standard RF head-coil. A total of 10 axial slices were oriented superior to inferior from the brain vertex, onto a midsagittal scout image, so as to include the primary sensorimotor cortex.

For the BOLD fMRI experiments, an in-house-developed gradient echo EPI technique (23) was used that acquired single-shot images with a matrix size of 64 × 64 over a field of view (FOV) of 240 × 240 mm^2. One additional EPI readout line was acquired as navigator to correct for ghosting artifacts (24) and signal phase fluctuations due to changes in B_0 over the course of the fMRI experiment. Only the data acquired on the flat portions of the EPI read-gradient were used, which constituted of 65% of the entire duration of the EPI train length. Slice thickness and slice gap were 4 mm and 1 mm, respectively, and the nominal in-plane resolution was 3.75 × 3.75 mm^2. Repetition time (TR) and flip angle were 3.0 seconds and 90°, respectively, a condition under which the contribution of inflow effects is expected to be small (25). The image acquisition bandwidth was 35 Hz per pixel.

Across the functional runs, the echo time was varied from 30 to 80 msec (30 to 200 ms for the three subjects) in a randomized time order, with steps of 5 msec (in the range: 30–50 msec), 10 msec (in the range: 50–140 msec), and 20 msec (in the range: 140 to 200 msec). Furthermore, on each subject, the image acquisition bandwidth was varied between effective values of 35 Hz and 17 Hz per pixel by using EPI trains of 40 and 80 msec in length, respectively. Maximum gradient strength and slew-rate were 12.2×10^{-3} T m^{-1} and 150 T m^{-1}second^{-1}, respectively, for the 35 Hz bandwidth, and 6.1×10^{-3} T m^{-1} and 38 T m^{-1}second^{-1} for the 17 Hz bandwidth. Bandwidth variation was done only at TE values of 50 and 60 msec. For anatomical reference, high-resolution T_1-weighted spin-echo images (matrix = 256 × 256, FOV = 240 mm, thickness = 4 mm, gap = 1 mm, TR = 600 msec, TE = 16 msec) were also acquired at the same location as the functional images.

Activation Paradigm

During the functional runs, subjects performed a sequential finger-tapping task, cued by a visual stimulus projected onto a screen and paced at 2 Hz. All subjects except one were strongly right handed and all performed the task with the dominant hand. Although all subjects were familiar with the task, one training session was administered during the prescanning for scanner adjustments and slice prescription procedures. The experimental paradigm consisted of four repetitive cycles (ON–OFF) during which the subjects switched between rest and finger tapping every 30 seconds. A total of 82 time-points were collected for each TE in a total scan time just over 4 minutes.

Data Analysis

fMRI data were analyzed off-line on a Linux workstation using the Interactive Data Language (RSI Inc.) and MEDx (Sensor Systems, VA) software. Image reconstruction and motion correction by spatial registration were performed using home-written software based on established code for registration (26,27). To facilitate the comparison of runs performed under the various conditions, all EPI images were normalized to their respective thermal noise levels, as determined from a region of interest (ROI) containing about 20 pixels outside of the brain and free of image artifacts. The thermal (intrinsic) noise levels were calculated as the average of

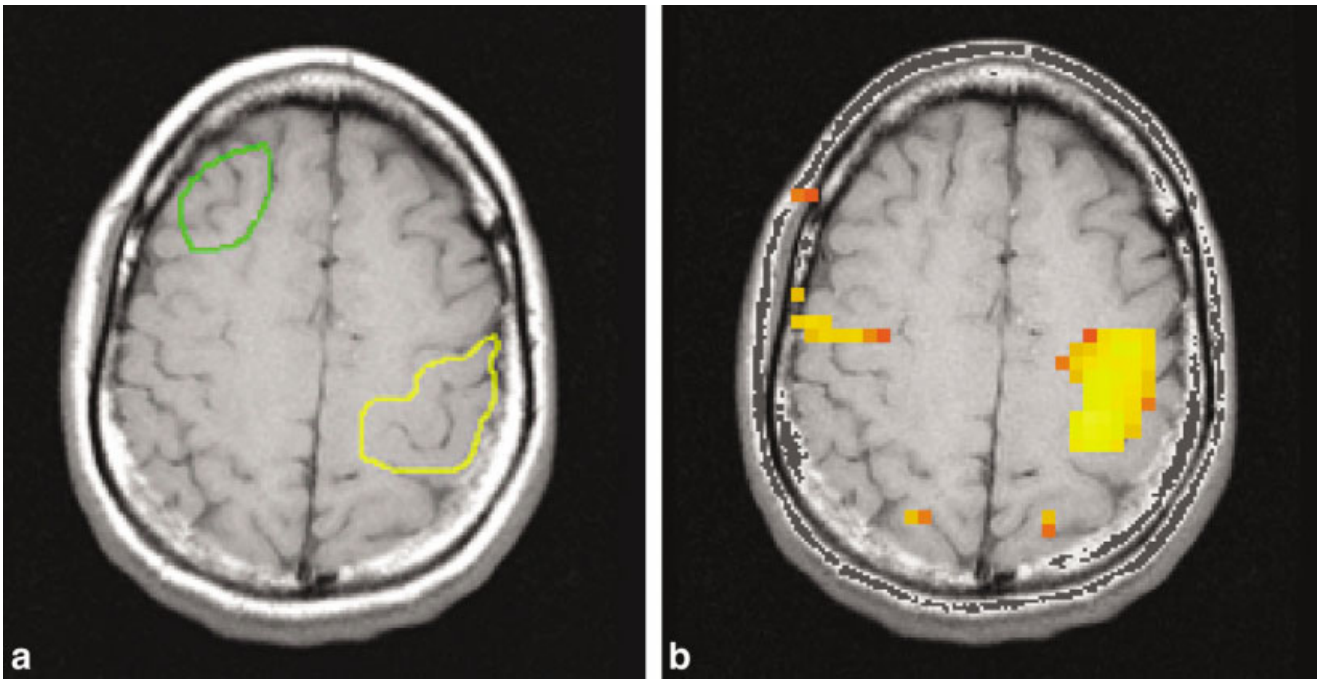

Figure 1. Example of anatomical preselection of primary sensorimotor cortex (yellow) and prefrontal cortex (PFC, green) ROIs for measurement of activation signal and noise (**a**). The selection was performed on a high resolution T1-weighted image, aligned with the functional data. The actual activation *t*-map (1.5 T, TE = 60 msec) is shown in (**b**).

the temporal SD of each pixel within the ROI, and included a Rayleigh correction to account for effects of noise rectification in magnitude images. As expected, thermal noise levels were constant across TE values, but not across bandwidths.

For each subject, obvious motion artifacts were assessed by inspection of the image intensity time-course of a few randomly chosen pixels. In addition, the presence of potential motion artifacts was evaluated by inspecting the motion correction parameters from the spatial registration routine. As it turned out, no corrections exceeding 2 mm were made on any of the runs and none of the subjects were excluded from further analysis.

To determine the activated voxels in each run, a multilinear regression analysis was performed, which included a modeled hemodynamic response curve based on the activation paradigm (a truncated Gaussian function with an σ of 3.5 seconds and a delay from stimulus to the top of the response of 5 seconds) and a linear function to model signal drift that was sometimes present in the time-series data. The statistical activation threshold was set at $P = 0.05$ after Bonferroni correction, based on the size of the preselected regions of interest. This resulted in *t*-thresholds ranging from 3.62 to 3.72.

Further analysis was aimed at determining ROIs to compare activation across the different runs performed under the various conditions described above. A single activation-based ROI across TEs and bandwidths was generated, based on the combination of activated areas from each run (28). This involved the following steps:

1. On each subject, an anatomical region encompassing the primary sensorimotor cortex (including M1 and S1) contralateral to the dominant hand was selected based on established landmarks (29,30) using the T_1-weighted images (Fig. 1). This region extended through the four to five slices that best exposed the motor cortex and was traced along the central sulcus encompassing both the precentral and the postcentral gyri, yielding a total volume of ~200 voxels, depending on the subject's anatomy. In order to minimize potential susceptibility problems, pixels at the edge of the brain were not included in the ROI. The ROI selection was done separately for 1.5 T and 3.0 T data.
2. A ROI was generated based on all voxels within the preselected primary sensorimotor cortex region that were statistically activated in any of the runs. This was done separately for the 1.5 T and the 3.0 T studies.
3. Only voxels that were in ROI's as defined in items 1 and 2 were subject to further analysis. In the following this region is indicated by sensorimotor cortex (SMC).

Subsequently, the average *t*-score, the mean activation signal, and the temporal noise level (SD over time) in SMC, as well as the total number of activated voxels were calculated for each subject, field strength, TE, and bandwidth. For comparison, the temporal noise level was also determined in an anatomical ROI over the prefrontal cortex (PFC), ipsilateral to the dominant hand (Fig. 1), and in an ROI from a region outside the brain. Lastly, estimates of T_2^* relaxation times were derived from the SMC ROIs using a single exponential fit to the TE-dependent signal strength.

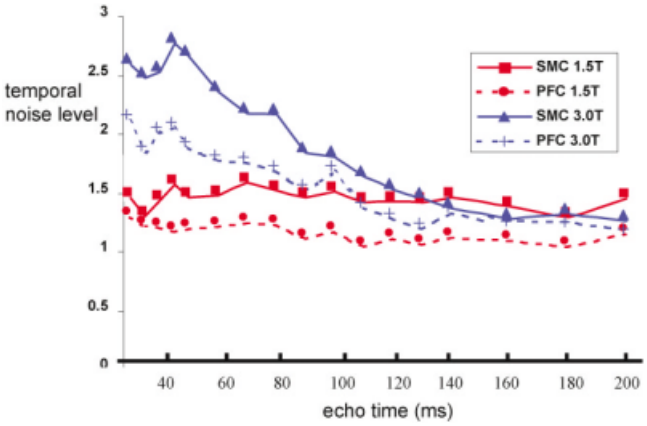

Figure 2. Average noise in SMC (solid lines) and PFC areas (dotted lines) as a function of TE, at 1.5 T (red) and 3.0 T (blue). Noise levels scaled to the intrinsic (thermal) noise level at each field.

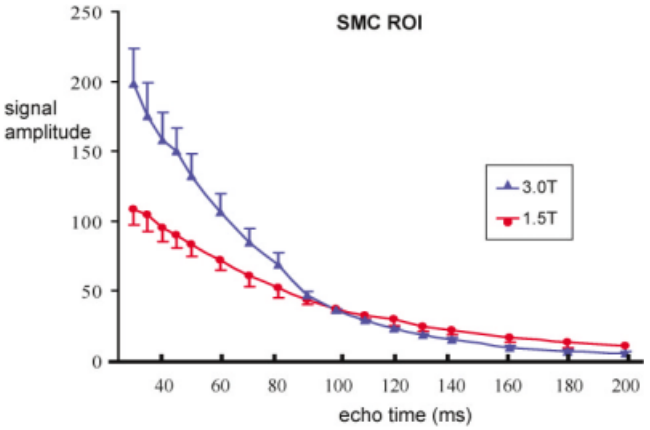

Figure 3. Dependence of SMC brain signal on TE at 1.5 T (red) and 3.0 T (blue). Signal amplitudes were averaged over al subjects, and scaled to intrinsic noise level at each field. Error bars indicate the positive (3.0 T) or negative (1.5 T) half of the SD.

RESULTS

Signal and Noise

The temporal noise levels in the ROIs chosen from a region outside the brain were independent of TE at both field strengths, confirming the expectation that it reflects thermal noise exclusively. Temporal noise levels in SMC and PFC areas, which reflected a combination of thermal and physiologic noise sources, are given in Fig. 2, scaled to thermal noise levels measured at each field and averaged over all scan sessions.

At 1.5 T, temporal noise levels in all areas showed weak TE dependence, with a trend towards lower noise at longer TEs. Averaged over all TEs, these noise levels were 45.0% and 15.5% above thermal noise in SMC and PFC areas, respectively.

At 3.0 T, temporal noise levels in SMC and PFC areas generally decreased with TE and were on average higher than at 1.5 T (95.6% and 59.1% above thermal noise, respectively). In the SMC area, there was a slight increase in temporal noise going from TE = 30 msec to TE = 45 msec, after which there was a general downward trend. Maximum temporal noise levels were 117.1% and 112.5% above thermal noise in SMC and PFC areas, respectively.

The TE dependence on brain signal amplitude, relative to thermal noise and averaged over all scan sessions is given in Fig. 3. At TEs below 110 msec, the 3.0 T signal was higher than the 1.5 T signal, and reached a maximum that is 93.6% higher than the 1.5 T maximum at the shortest echo time (TE = 30 msec).

T_2* values were 73.2(±9.9) msec and 48.9(±5.1) msec at 1.5 T and 3.0 T, respectively, as estimated from the average of single exponential fits to the TE-series data of the individual scan sessions.

At the lower bandwidth of 17 Hz per pixel, brain signal levels (relative to intrinsic noise) were 25% and 15% higher compared to the 35 Hz per pixel bandwidth at 1.5 T and 3.0 T, respectively. This was somewhat below the 41% improvement expected based on theoretical grounds, in absence of T_2* relaxation and image artifacts. Temporal noise levels increased at the lower bandwidth, in particular at 3.0 T. The increases were 14% and 22% at TE = 50 msec and TE = 60 msec, respectively.

fMRI Sensitivity

The motor task elicited a strong BOLD response in the primary sensorimotor cortex in all subjects. The activation maps generated with identical statistical thresholds ($P < 0.05$, Bonferroni corrected) showed a consistently greater extent of activation in the 3.0 T than in the 1.5 T data, except for TEs longer than 130 msec. Results of the fMRI experiments at varying TE are given in Figs. 4, 5 and 6, showing extent of activation, amplitude of activation, and average *t*-score, respectively. At each field strength, the three quantities showed similar trends.

At 1.5 T, the number of activated voxels (Fig. 4) reached a relatively broad maximum at TEs between 50–160 msec, with a rapid dropoff outside this range. The extent of activation found at 3.0 T was generally much larger ($P < 0.0007$ within the range of TEs of

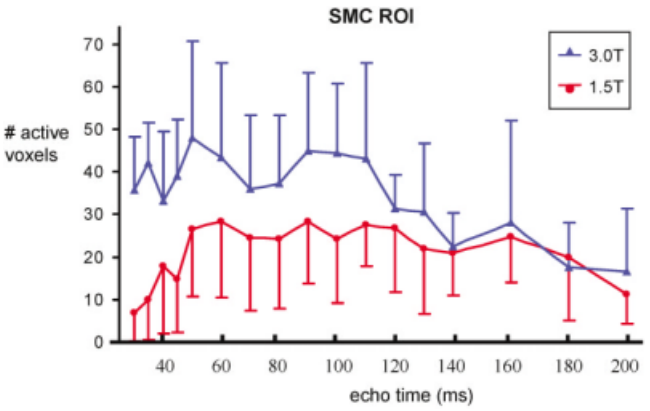

Figure 4. Spatial extent of SMC activation as function of TE. At the TEs optimal for the individual field strengths, the number of active voxels is about 61% larger at 3.0 T as compared to 1.5 T ($P < 1.75 \times 10^{-6}$). Error bars indicate the positive (3.0 T) or negative (1.5 T) half of the SD.

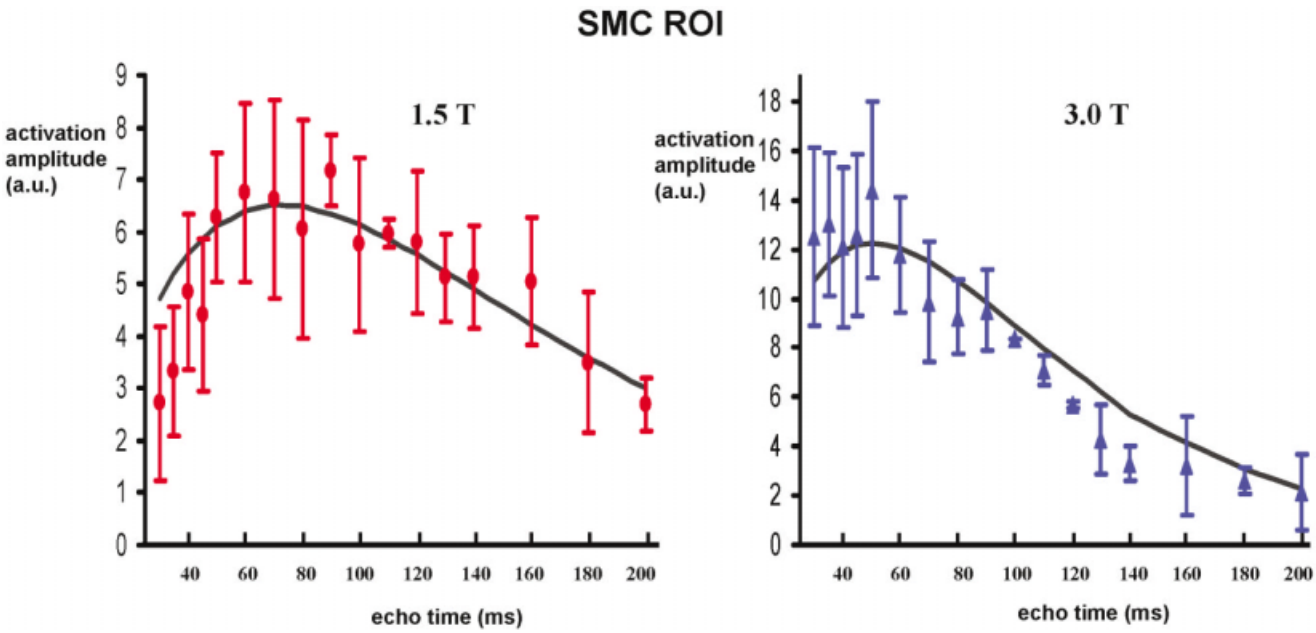

Figure 5. Measured and simulated average amplitude of SMC activation as function of TE at 1.5 T (**a**, red) and 3.0 T (**b**, blue), averaged over scan sessions. Maximum activation signal was found around TE = 70 msec (1.5 T) and around TE = 50 msec (3.0 T). Solid lines represent fit to single exponential model of T_2* relaxation. Error bars indicate SD.

30–130 msec), with a broad optimum found at TEs between 30 and 110 msec. At the optimal TEs for each field strength, the averaged number of activated voxels was about 58.7% larger at 3.0 T as compared to 1.5 T.

Although the number of activated voxels contains some information about fMRI sensitivity, its use for comparing relative performance of activation experiments has a number of drawbacks. One drawback is the limited dynamic range due to the fact that above a certain minimum sensitivity, all activated cortex will pass threshold, after which the number of voxels passing threshold is not expected to increase with increased sensitivity.

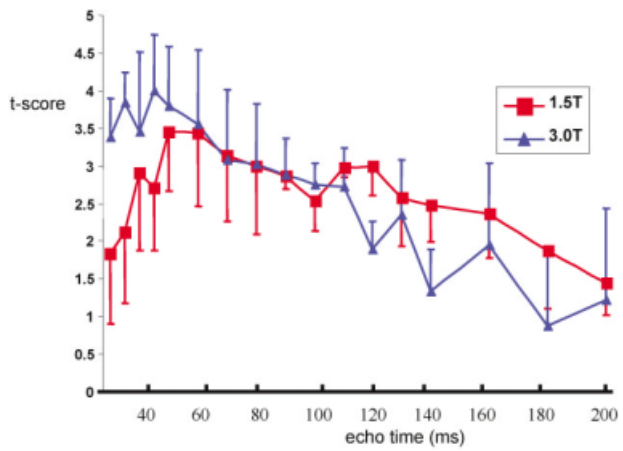

Figure 6. Statistical *t*-score as a function of TE, averaged over activated voxels in SMC in all scan sessions. The *t*-scores had a broad optimum around TE = 45 msec (t = 4.0) and at TE = 50–60 msec (t = 3.4) for the 3 T and the 1.5 T data, respectively. At TEs below 60 msec, the average *t*-score at 3.0 T is significantly higher than at 1.5 T ($P < 0.01$). Error bars indicate the positive (3.0 T) or negative (1.5 T) half of the SD between sessions.

The amplitude of activation (Fig. 5) found at 3.0 T was generally higher (74.9% averaged over all TEs) than that at 1.5 T. Simulating the MRI signal behavior as a single exponential signal decay, with resting T_2* values of 73.2 and 48.9 msec at 1.5 and 3.0 T, respectively, and an increase in T_2* to 75.3 and 49.6 msec, respectively during activation, the measured signal behavior could be reproduced reasonably well (Fig. 5). The simulations somewhat overestimated the activation amplitude at short TE at 1.5 T, and at the longer TEs at 3.0 T. The maximum of the fit to the 3.0 T data (at TE = 47 msec) was 92% higher than the 1.5 T maximum (TE = 70 msec).

The *t*-scores averaged over the activated voxels in all scan sessions (Fig. 6) reached maxima of 3.4 (TE = 50–60 msec) and 4.0 (TE = 45 msec) at 1.5 and 3.0 T, respectively. The TE range for optimum *t*-score was very broad at both fields and was within 20% of optimum in a TE range of 50–160 msec at 1.5 T and 30–110 msec at 3.0 T. At TEs below 60 msec, the average *t*-score at 3.0 T was significantly higher than at 1.5 T ($P < 0.0095$). Between TE = 60 msec and TE = 110 msec, average *t*-scores were similar at both fields, whereas beyond TE = 110 msec, 1.5 T *t*-scores were higher than the 3.0 T values ($P < 0.004$).

The effects of bandwidth on fMRI measures are given in Table 1. Despite the increase in MRI signal at lower bandwidth, extent and significance of activation were not, or at best, marginally increased. At 1.5 T, the extent of activation was slightly reduced, whereas the average *t*-score in this area improved slightly, but not significantly (1.2%, $P < 0.1$). At 3.0 T, both the extent of activation (13%, $P < 0.006$) and *t*-scores (7.0%, $P < 0.01$) were reduced at the lower bandwidth.

Table 1
Variation of EPI Acquisition Bandwidth

	1.5 T data				3 T data			
TE (msec)	50		60		50		60	
Bandwidth	35 Hz	17 Hz	35 Hz	17 Hz	35 Hz	17 Hz	35 Hz	17 Hz
T-score	3.45	3.68	3.39	3.65	3.80	3.41	3.55	3.16
SMC signal amplitude	84.2	106.6	72.1	91.7	98.3	120.6	79.11	97.55
PFC signal amplitude	89.0	111.3	76.8	97.3	94.99	126.17	78.21	104.17
Temporal noise	1.46	1.53	1.48	1.55	2.66	3.02	2.36	2.89
No. activated voxels	27.8	26.9	27.8	25.7	47.5	38.6	40.6	36.6

DISCUSSION

The results of our EPI BOLD fMRI motor activation experiments showed that the largest activation signal in the SMC at 1.5 T and 3.0 T is achieved at between TE = 50 and 60 msec and around TE = 45 msec, respectively. These TEs are close to the respective tissue T_2* values at both fields, consistent with theory based on single exponential signal decay, and consistent with results of previous studies (20).

Where 1.5 T data showed noise levels almost independent of TE, at 3.0 T, temporal noise levels (Fig. 2) were generally found to decrease with TE. This downward trend with TE is attributed to head motion and to physiologic noise sources, such as tissue pulsations related to cardiac and respiratory cycles (9,22), which usually scale with image intensity level. Furthermore, the increase in temporal noise in SMC at TE = 45 msec, is consistent with the presence of BOLD effects not correlated with the activation model (18,22). The latter should result in increased noise levels around TE = T_2*.

Because of the substantial contribution of TE-dependent noise at 3.0 T, the overall sensitivity of the fMRI experiment in terms of average *t*-score over a given area of activation did not follow theoretical predictions based on amplitude of activation alone (5). The decreasing noise levels at longer TEs led to a broadening of the *t*-score vs. TE curve towards longer TEs (Fig. 6), and a nearly constant *t*-score for TEs in the range of 30–110 msec. This was not the case at 1.5 T, where the thermal noise contribution was higher, a minimal TE dependency of the noise level was observed, and *t*-scores showed a TE dependence that was similar to that of the activation amplitude.

Despite increased intrinsic SNR at 3.0 T, the ROI-averaged *t*-scores for 1.5 T and 3.0 T were rather similar. This is partly due to the increased temporal noise at 3.0 T, and partly due to the fact that the active ROI (SMC area) included a larger number of voxels at 3.0 T. The extra voxels at 3.0 T are likely to have relatively low *t*-scores and skew the average *t*-score towards lower values.

Reduction of the acquisition bandwidth did not give the gain in *t*-score that could be expected based on sensitivity issues (i.e., signal amplitude levels relative to thermal noise). The increase in *t*-scores at 1.5 T was only 1.2%, whereas bandwidth reduction led to a 7% loss in *t*-scores at 3.0 T. An explanation is that signal gains with bandwidth reduction are partially offset by reduction in activation amplitude (because of increased departure from optimum TE), possible increased blurring, and an increase in physiologic noise. Note that blurring effects are increased at 3.0 T due to the shorter T_2* compared to 1.5 T. For equivalent blurring and geometric distortions at both field strengths, one would have to make the bandwidth at 3.0 T 50% and 100% higher, respectively, assuming blurring to scale with T_2* and geometric distortions to scale with field strength. The effects of bandwidth reduction might be different at higher spatial resolution (i.e., reduced voxel size), depending on the contribution of physiologic noise relative to that of intrinsic noise.

Increasing the spatial resolution beyond the 4 mm cubic resolution investigated in this work could change the outcome of the results. At higher spatial resolutions, the relative role of physiologic noise is ultimately reduced, possibly resulting in increased benefits of 3.0 T over 1.5 T. Furthermore, at higher resolution, baseline T_2* is likely to increase due to the reduction in signal dephasing, caused by macroscopic susceptibility effects. At this point, the overall effect of resolution on optimum TE is unclear. Measurement of T_2* in the superior brain at 4, 2, and 1 mm cubic resolution show no dramatic variation in global T_2* values, although, at 3.0 T, locally significant differences are observed, especially in the presence of CSF spaces and larger veins (Fig. 7, unpublished data from a separate experiment). This is attributed to macroscopic susceptibility effects.

The results presented above are not directly extendable to other brain areas, where anatomy and physiology, as well as magnetic properties of tissues (including apparent T_2*) are different. On the other hand, a study of motor, visual, and auditory cortices at 3.0 T (21) showed that the differences in optimum TE between the different anatomical areas were small (between 30 and 45 msec for both motor and auditory cortices, and between 25 and 30 mec for the visual cortex); this suggests some extendibility of the results presented above.

To some extent, the results presented in this work are dependent on the type of filtering used to suppress physiologic noise. In the ideal case, all physiologic noise sources are modeled and incorporated in the analysis. The linear detrending used in the experiments described above is only a first approximation, which removes most of the 1/f–like noise (31) present in fMRI experiments. Signal fluctuations related to cardiac and respiratory cycles, and neuronal activity uncorrelated with the activation paradigm (in particular during "rest" stages) was not effectively removed in our analysis. These noise sources are likely to affect fMRI sensitivity, in particular in situations with high intrinsic SNR (low spatial resolution, low bandwidth, short TE, or high

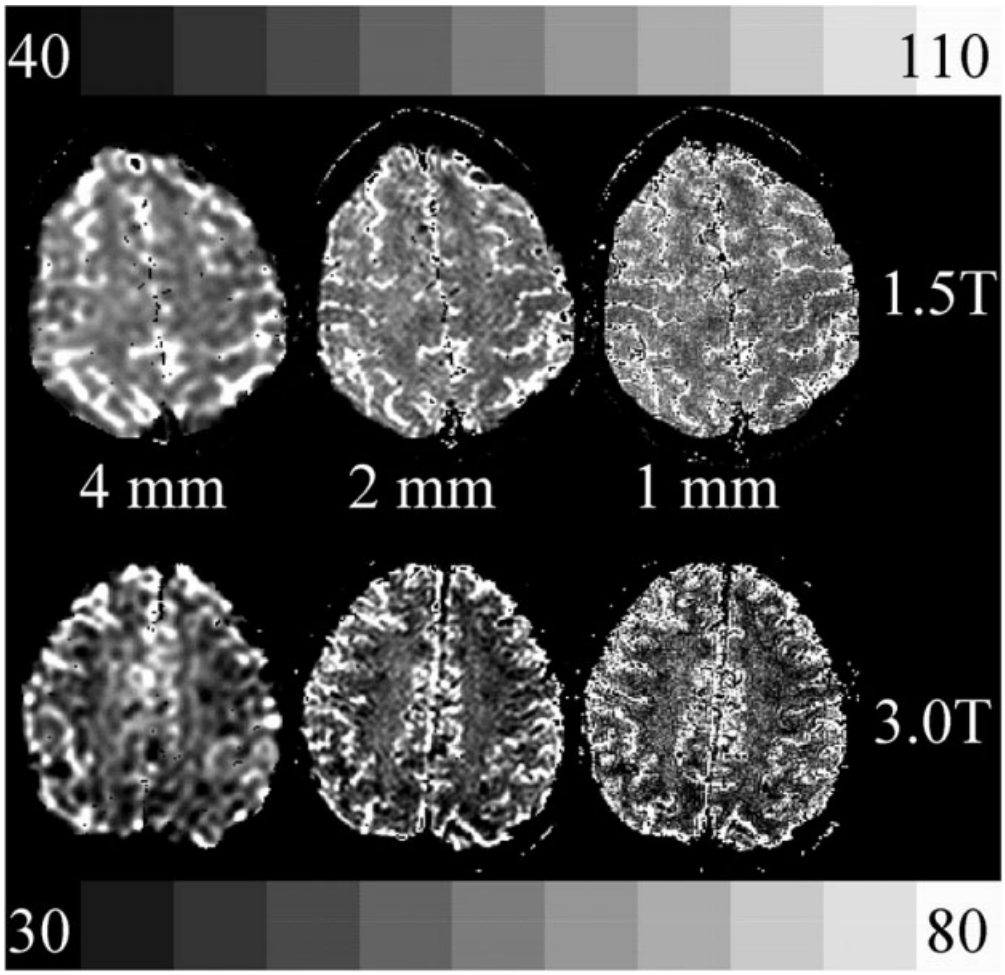

Figure 7. Dependence of T_2* on resolution. T_2* maps were calculated at 4, 2, and 1 mm (cubic) resolution from gradient echo MRI data in superior brain. Global T_2* values do not dramatically increase at higher resolution. At 3.0 T, the 4 mm resolution data shows more distinct local dark spots, attributed to macroscopic susceptibility effects.

field). Especially under these conditions, it is important to accurately model the noise sources, or to reduce their influence by filtering or by careful design of stimulation paradigms.

REFERENCES

1. Ogawa S, Lee TM, Kay AR, Tank DW. Brain magnetic resonance imaging with contrast dependent on blood oxygenation. Proc Natl Acad Sci USA 1990;87:9868–9872.
2. Logothetis NK, Pauls J, Augath M, Trinath T, Oeltermann A. Neurophysiological investigation of the basis of the fMRI signal. Nature 2001;412(6843):150–157.
3. Tootell RB, Hadjikhani NK, Vanduffel W, et al. Functional analysis of primary visual cortex (V1) in humans [Review]. Proc Natl Acad Sci USA 1998;95:811–817.
4. Menon RS, Ogawa S, Tank DW, Ugurbil K. Four Tesla gradient recalled echo characteristics of photic stimulation induced signal changes in the human primary visual cortex. Magn Reson Med 1993;30:380–386.
5. Van Gelderen P, Duyn JH, Liu GY, Moonen CT. Optimal T2* weighting for BOLD functional MRI of the human brain. Proc Indian Acad 1994;106:1617–1624.
6. Bandettini PA, Wong EC, Jesmanowicz A, Hinks RS, Hyde JS. Spin-echo and gradient-echo EPI of human brain activation using BOLD contrast: a comparative study at 1.5 T. NMR Biomed 1994; 7:12–20.
7. Glover GH, Lemieux SK, Drangova M, Pauly JM. Decomposition of inflow and blood oxygen level-dependent (BOLD) effects with dual-echo spiral gradient-recalled echo (GRE) fMRI. Magn Reson Med 1996;35:299–308.
8. Yang Y, Glover GH, van Gelderen P, et al. Fast 3D functional magnetic resonance imaging at 1.5 T with spiral acquisition. Magn Reson Med 1996;36:620–626.
9. Bandettini PA, Wong EC, Jesmanowicz A, et al. MRI of human brain activation at 0.5T, 1.5T and 3.0T: Comparison of ΔR2* and functional contrast to noise ratio. In: Proc Soc Magn Reson 1994;2:434. (abstract)
10. Thulborn KR, Chang SY, Shen GX, Voyvodic JT. High-resolution echo-planar fMRI of human visual cortex at 3.0 tesla. NMR Biomed 1997;10:183–190.
11. Krueger G, Kastrup A, Glover GH. Neuroimaging at 1.5 T and 3.0 T: comparison of oxygenation-sensitive magnetic resonance imaging. Magn Reson Med 2001;45:595–604.
12. Turner R, Jezzard P, Wen H, et al. Functional mapping of the human visual cortex at 4 and 1.5 Tesla using deoxygenation contrast EPI. Magn Reson Med 1993;29:277–279.
13. Menon RS, Goodyear BG. Submillimeter functional localization in human striate cortex using BOLD contrast at 4 Tesla: implications for the vascular point-spread function. Magn Reson Med 1999;41: 230–235.
14. Yang Y, Wen H, Mattay VS, Balaban RS, Frank JA, Duyn JH. Comparison of 3D BOLD functional MRI with spiral acquisition at 1.5 and 4.0 T. Neuroimage 1999;9:446–451.
15. Yacoub E, Shmuel A, Pfeuffer J, et al. Imaging brain function in humans at 7 Tesla. Magn Reson Med 2001;45:588–594.
16. Pfeuffer J, Van de Morteele PF, Adriany G, Hu X, Ugurbil K. Submillimeter event-related fMRI at high temporal resolution. In: Proc Intl Soc Magn Reson 2001;9:1257. (abstract)

17. Howseman AM, Grootoonk S, Porter DA, Ramdeen J, Holmes AP, Turner R. The effect of slice order and thickness on fMRI activation data using multislice echo-planar imaging. Neuroimage 1999;9: 363–376.
18. Hyde JS, Biswal BB, Jesmanowicz A. High-resolution fMRI using multislice partial k-space GR-EPI with cubic voxels. Magn Reson Med 2001;46:114–125.
19. Speck O, Hennig J. Functional imaging by I-0- and T-2*-parameter mapping using multi-image EPI. Magn Reson Med 1998;40:243–248.
20. Posse S, Wiese S, Gembris D, et al. Enhancement of BOLD-contrast sensitivity by single-shot multi-echo functional MR imaging. Magn Reson Med 1999;42:87–97.
21. Clare S, Francis S, Morris PG, Bowtell R. Single-shot T2* measurement to establish optimum echo time for fMRI: Studies of the visual, motor, and auditory cortices at 3.0 T. Magn Reson Med 2001;45:930–933.
22. Krueger G, Glover GH. Physiological noise in oxygenation-sensitive magnetic resonance imaging. Magn Reson Med 2001;46:631–637.
23. Yang Y, Glover GH, van Gelderen P, et al. A comparison of fast MR scan techniques for cerebral activation studies at 1.5 tesla. Magn Reson Med 1998;39:61–67.
24. Bruder H, Fischer H, Reinfelder HE, Schmitt F. Image reconstruction for echo planar imaging with non-equidistant k-space sampling. Magn Reson Med 1992;23:311–323.
25. Gao JH, Miller I, Lai S, Xiong J, Fox PT. Quantitative assessment of blood inflow effects in functional MRI signals. Magn Reson Med 1996;36:314–319.
26. Thevenaz P, Ruttimann UE, Unser M. Iterative multi-scale registration without landmarks. In: Proc IEEE International Conference on Image Processing 1995;3:228–231. (abstract)
27. Unser M, Aldroubi A, Gerfen CR. A multiresolution image registration procedure using spline pyramids. In: Proc SPIE, 1993;2034: 160–170. (abstract)
28. Waldvogel D, van Gelderen P, Meullbacher W, Ziemann U, Immisch I, Hallett M. The relative metabolic demand of inhibition and excitation. Nature 2000;406:995–998.
29. Yousry TA, Schmid UD, Jassoy AG, et al. Topography of the cortical motor hand area: prospective study with functional MR imaging and direct motor mapping at surgery. Radiology 1995; 195:23–29.
30. Naidich TP, Valavanis AG, Kubik S. Anatomic relationships along the low-middle convexity: Part I—Normal specimens and magnetic resonance imaging. Neurosurgery 1995;36:517–532.
31. Zarahn E, Aguirre GK, D'Esposito M. Empirical analyses of BOLD fMRI statistics. I. Spatially unsmoothed data collected under null-hypothesis conditions. Neuroimage 1997;5:179–197.